



Surface modifications of TiN coating by the pulsed TEA CO₂ and KrCl laser

Milan S. Trtica^{a,*}, Biljana M. Gaković^a, Ljubica T. Petkovska^a, Victor F. Tarasenko^b,
Andrei V. Fedenev^b, Eugenii I. Lipatov^b, Mikhail A. Shulepov^b

^a*Vinča Institute of Nuclear Sciences, P.O. Box 522, 11001 Belgrade, Yugoslavia*

^b*High Current Electronics Institute SB of RAS, 4 Akademicheskii Avenue, Tomsk 634055, Russia*

Received 18 June 2003; accepted 23 October 2003

Abstract

Interaction of a transversely excited atmospheric (TEA) CO₂ and excimer-KrCl laser, pulse duration $\sim 2 \mu\text{s}$ (FWHM of initial spike $\sim 100 \text{ ns}$) and $\sim 12 \text{ ns}$ (FWHM), respectively, with polycrystalline titanium nitride (TiN) coating deposited on high quality steels, was studied. The results have shown that the titanium nitride was surface modified by the laser beam, with an energy density (ED) of 43.0 J/cm^2 (TEA CO₂ laser system) and 3.3 J/cm^2 (KrCl system), respectively. The energy absorbed from the CO₂ laser beam is partially converted to thermal energy, which generates a series of effects such as melting, vaporization of the molten material, shock waves, etc. The energy from the excimer-KrCl laser primarily leads to a fast and intense target evaporation. Calculated maximal temperatures, on the target surface, were 3940 and 8000 K for the TEA CO₂ and the KrCl lasers, respectively. It is assumed that TEA CO₂ laser affects the target deeper, during a longer time than the KrCl laser. The effects of the KrCl laser are confined to a localized area, near target surface, in the course of short time.

The following morphological changes of titanium nitride surface were observed: (i) both types of laser caused ablation of the TiN coating in the central zone of the irradiated area, (ii) appearance of a hydrodynamic feature like resolidified droplets of material in the surrounding outer zone (cracking) in the case of the TEA CO₂ laser, and (iii) appearance of wave-like microstructures (consisting of periodic parallel fringes with a period of about 20 microns) in the case of KrCl laser. Formation of the wave-like microstructures is discussed in the context of laser-induced periodic surface structure (LIPSS) effects and diffraction phenomena.

The process of the CO₂ and KrCl laser interaction with titanium nitride were typically accompanied by plasma formation. Plasma appeared above the target after about 40 and 1 laser pulse, respectively.

© 2003 Elsevier B.V. All rights reserved.

Keywords: Laser surface modification; TiN coating; Laser-induced periodic microstructure; Pulsed TEA carbon-dioxide laser; Pulsed excimer-KrCl laser

1. Introduction

Surface modification studies of titanium-based ceramic coatings, especially titanium nitride (TiN)

deposited on the steel substrate, by various types of energetic beams, including the laser beam, are of a great fundamental and technological interest.

Titanium nitride exhibits extraordinary physical and chemical properties: high melting point, thermodynamic stability, high hardness, etc. [1]. It is therefore very attractive in microelectronics, tool protection industry, as well as in nuclear and sensor technologies,

* Corresponding author. Tel.: +381-11-2453-967;

fax: +381-11-344-0100.

E-mail address: etrtica@vin.bg.ac.yu (M.S. Trtica).

etc. The interest in studies of laser beam interaction with titanium nitride has relatively risen, especially in the last decade. The Ruby-[2], Nd:YAG-[3], Ti:Sapphire-[4], excimer-XeCl-[5], and CO₂-[6,7] laser beams have so far been employed for these purposes.

The interaction of a pulsed CO₂ or KrCl laser beam with titanium nitride has not been sufficiently described in literature [6–8]. The present paper deals with the effects of a pulsed transversely excited atmospheric (TEA) CO₂ laser emitting in the IR region (~10 μm) and the excimer-KrCl laser (UV region, 0.222 μm) on polycrystalline titanium nitride coatings deposited on high quality steels. Special attention was

paid to the morphological surface modifications of TiN for both types of pulsed laser radiation.

2. Experimental

The TiN coatings (thickness, 1 μm) used in the experiment were deposited on a steel substrate via reactive dc magnetron sputtering of a titanium target (99.9%) by Ar ions in nitrogen atmosphere [9]. The substrates, (steel type AISI M2 or AISI 316), were prepared by the standard metallographic procedure. This included polishing, rinsing, and drying.

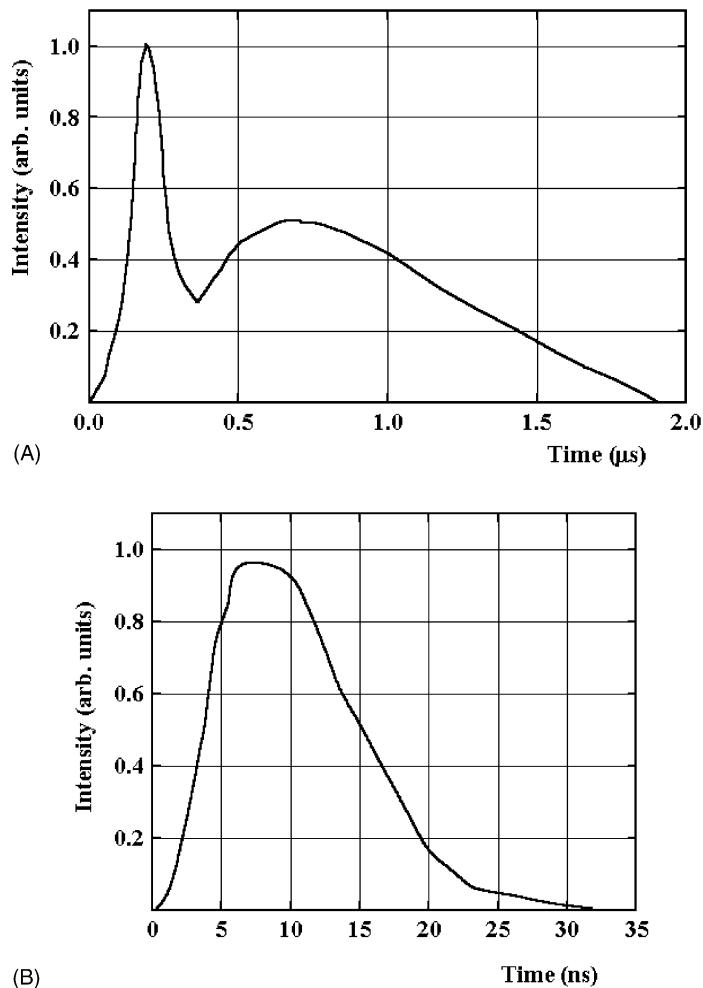


Fig. 1. Temporal shape of the TEA CO₂ (A) and KrCl (B) laser pulses. (Horizontal scales—0.2 μs/div (A) and 5 ns/div (B). FWHM: ~100 ns (of the first peak) and ~12 ns, respectively).

Bulk dimensions of rectangularly shaped substrates were typically 15 mm × 10 mm × 3 mm.

Sample irradiations were performed with laser beams focused by a KBr/quartz lens, for the TEA CO₂/KrCl laser radiation, focal lengths 6.0 and 10 cm, respectively. In the case of the KrCl laser, an aperture diaphragm of 5 mm diameter located in front of the quartz lens was used to form a circular laser spot on the target surface. The angle of incidence of the laser beam with respect to the surface was 90°. The irradiation was carried out in air, at a pressure of 1013 mbar and relative humidity of 60%.

The TEA CO₂ laser was used running in the transverse fundamental mode or the multimode regime, whereas KrCl laser operated only in the TEM₀₀ mode.

Conventional (1 atm) CO₂/N₂/He gas mixtures were used for the TEA CO₂ laser [10] yielding pulses with a gain switched peak followed by a slowly decaying tail, see Fig. 1A.

The KrCl excimer laser was operated with typical HCl/Kr/Ne gas mixtures [11] at higher pressures of about 3 atm. A typical shape of the laser output pulses is given in Fig. 1B.

Detailed characteristics of the lasers used in the experiments are given in Table 1.

Various analytical techniques were used for characterization of the samples. X-ray diffraction (XRD) was employed for identifying crystal phases, growth orientation, etc. Surface morphology was monitored by optical microscopy (OM). Nontypical analysis

methods were also used: atomic force microscope (AFM) and scanning electron microscopy (SEM) with secondary electron (SE) and back-scattered electron (BSE) detectors.

3. Results and discussion

X-ray diffraction analysis of TiN coating prior to laser irradiation has confirmed its polycrystalline structure. The coating showed cubic B1 structure of the NaCl-type with prominent (1 1 1) and (2 2 0) orientations. Cross-section analysis of the coating has shown columnar crystal structure. The TiN coating was golden-yellow colored, typical for a [Ti]/[N] = 1 stoichiometric composition.

Investigation of the laser induced TiN morphological changes has shown their dependence on beam characteristics: primarily on the energy density, peak power density, pulse duration, number of pulses and wavelength.

Morphological changes of the TiN for 1, 20, and 500 cumulated laser pulses, TEA CO₂ laser, and for 20 and 500 subsequent pulses in the case of the KrCl system are presented in Figs. 2, 3 and 5, respectively. Energy densities of laser radiation of 43.0 J/cm² (TEA CO₂ laser) and 3.3 J/cm² (KrCl system) induce significant surface modifications of the TiN surface. The induced modifications can be presented as follows.

3.1. TEA CO₂ laser

After 1 and 20 pulses at 43.0 J/cm² (Fig. 2B and C) the damage of the TiN coating can be clearly recognized. In the central part of the damaged area, cracks were already found after the first pulse, Fig. 2B1, while the TiN layer on the AISI M2 substrate was completely removed after 20 pulses, Fig. 2C2. On the periphery of the damaged zone, hydrodynamic effects become visible after about 20 accumulated pulses, Fig. 2C1. After 500 pulses (Fig. 2D) the following effects are observed: (i) ablation of the TiN coating in the central zone, (ii) appearance of cracking and hydrodynamic effects of the steel substrate in the central zone, and (iii) appearance of four almost concentric outer damage zones with hydrodynamic features like resolidified droplets of materials (Fig. 2D2).

Table 1

Typical experimental conditions for used TEA CO₂ and KrCl laser

The type of laser system	TEA CO ₂ laser	KrCl laser
Gas mixture	CO ₂ /N ₂ /He	HCl/Kr/Ne
Operational gas mixture pressure (atm)	1	3
Output pulse energy (mJ)	to 85	to 8
FWHM ^a (ns)	~100 (initial spike)	~12
Mode structure	TEM ₀₀ /or multimode	TEM ₀₀
Peak power density (MW/cm ²)	to 150	to 280
Spectral emission ^b	10.5709 and 10.5909 μm	0.222 μm

^a Full width at a half maximum. The TEA CO₂ laser pulse, for difference from KrCl system, consists of an initial spike and a tail. The tail duration is about 2 μs.

^b Only the TEA CO₂ laser simultaneously operates at two wavelengths, i.e. 10.5909 and 10.590 μm, P(18) and P(20) transitions.

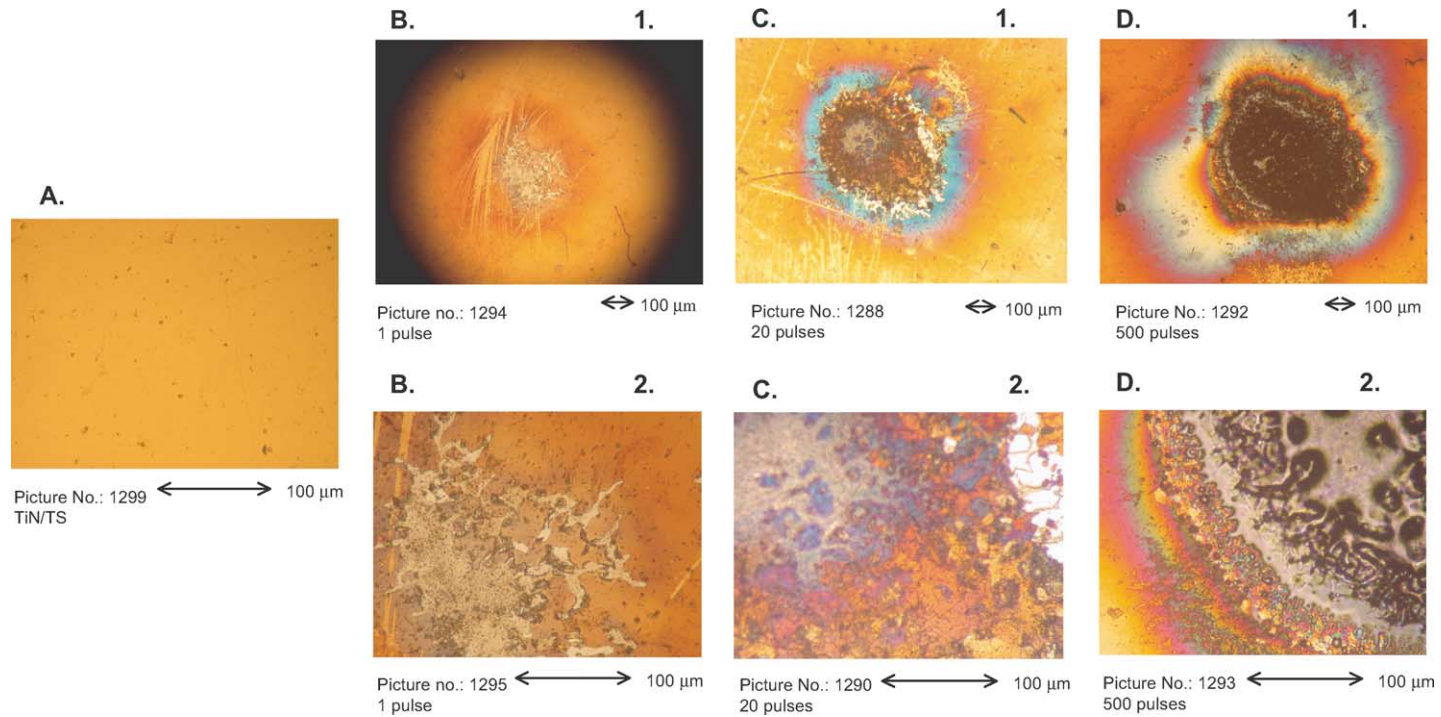


Fig. 2. TEA CO₂ laser-induced morphology changes of TiN coating (thickness, 1 μm)/Steel-AISI M2. Analysis was carried out by optical microscopy. Laser was operating in TEM₀₀ mode; pulse with tail—Fig. 1A; energy density, 43.0 J/cm². (A)—The view of TiN coating prior laser action; (B)—TiN coating after one laser pulse action ((B1, B2)—entire spot and periphery of damage area, respectively); (C)—TiN coating after 20 laser pulses action ((C1, C2)—entire spot and center of damage area, respectively); (D)—TiN coating after 500 laser pulse action ((D1, D2)—entire spot and periphery of the damage area, respectively).

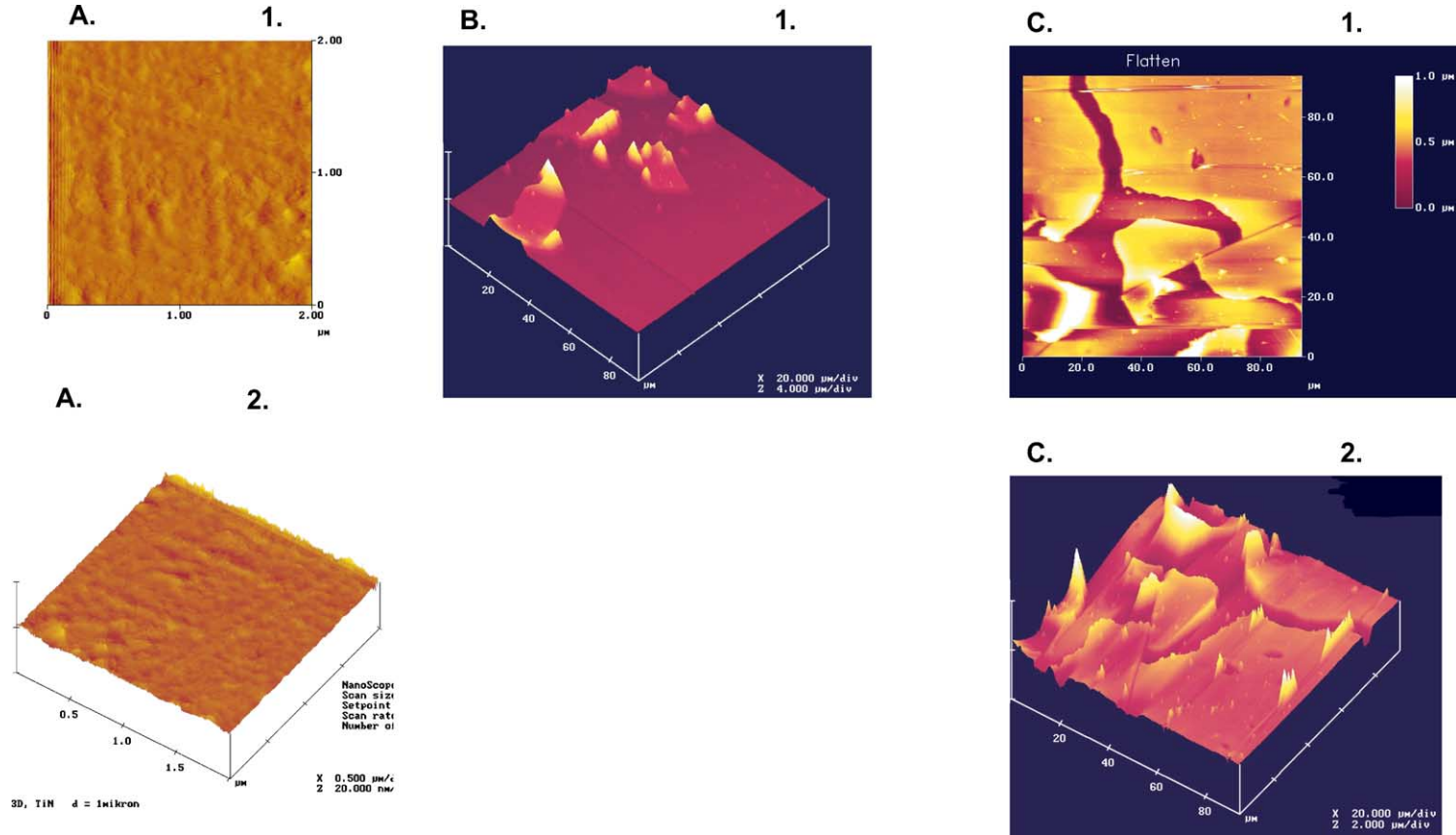


Fig. 3. TEA CO₂ laser-induced morphology changes of TiN coating (thickness, 1 μm)/Steel-AISI 316. Analysis was carried out by atomic force microscopy (AFM). Laser was operating in TEM₀₀ mode; pulse with tail—Fig. 1A; energy density, 43.0 J/cm². (A)—The view of TiN coating prior laser action; ((A1, A2)—two- and three-dimensional view, respectively); (B, C)—TiN coating after one laser pulse action ((B1)—center of the damage area; (C1, C2)—two- and three-dimensional view of periphery, respectively).

It should be pointed out that qualitatively comparable changes (like cracking, etc.) of the TiN coating occur (if deposited on AISI 316-steel substrates), see Fig. 3. The composition of steel-substrates AISI 316 and AISI M2 is given in [12].

The process of the TEA CO₂ laser interaction with TiN coating during the first pulses was not accompanied by appearance of plasma in front of the target. Spark-like plasmas were ignited after about 40 cumulated pulses.

Generally, the energy absorbed from the TEA CO₂ laser beam is assumed to be converted into thermal energy which causes melting, vaporization of the molten material, dissociation or ionization of the vaporized material, and shock waves in the vapor and the solid. The calculated surface temperature as a function of time for the laser pulse shape used (Fig. 1A) [13] was carried out by Eq. (1). This equation is reported in [14].

$$\Delta T(t) = \frac{A}{c\rho\sqrt{\pi\kappa}} \int_0^t \frac{I(\xi) d\xi}{\sqrt{t-\xi}} \quad (1)$$

Absorptivity is denoted by A , specific heat by c , thermal diffusivity by κ , target density by ρ , and the laser beam intensity by I . The equation was solved numerically. The model was first tested for a titanium target. The parameters for Ti, including laser energy density and pulse shape, were taken from [14]. The calculated temperature profile is in good agreement with [14]. For a given pulse shape of the TEA CO₂ laser with $I_{\max} = 150 \text{ MW/cm}^2$ and an absorptivity $A = 0.08$ the calculation yields the temporal temperature dependency shown in Fig. 4. After the first peak of about $0.2 \mu\text{s}$ the temperature slightly decays prior to reaching a maximum of 3940 K, approximately after $1.1 \mu\text{s}$ (corresponding to $\sim 2/3$ of the duration of the slowly decaying tail). Thus, it can be assumed that the energy of the laser sustained in the tail essentially affects surface modification of the target. It is interesting to note that the maximum temperature is greater than the decomposition temperature of TiN, which is about 3220 K.

3.2. KrCl laser

The KrCl laser radiation at an energy density of 3.3 J/cm^2 modified the TiN coating, although the

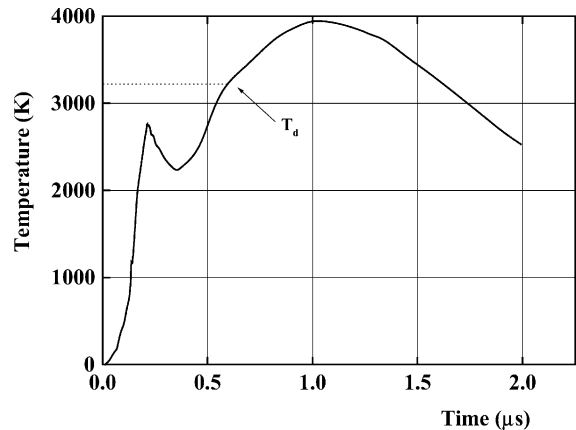


Fig. 4. Surface temperature variation of a sample during irradiation process with TEA CO₂ laser. (T_d denotes the decomposition temperature of the TiN coating).

ED was approximately by a factor of 13 lower than that of the TEA CO₂ laser. Irradiation of TiN coatings with 500 accumulated laser pulses resulted in a more pronounced surface modification than obtained with 20 pulses (Fig. 5). Changes on the surface can be summarized as follows: (i) ablation of the TiN coating in the central zone, Fig. 5B1,2 and C1,2, (ii) appearance of a periodical microstructure, particularly visible after 20 cumulated pulses, Fig. 5B2, and (iii) appearance of three damaged zones on the periphery, albeit without additional hydrodynamic features, Fig. 5C3.

Periodic microstructures were recorded in all cases, Fig. 5B1–3. These structures consist of numerous fringes of $20 \mu\text{m}$ estimated width. Creation of microstructures (MS) with a period close or different than the laser wavelength has been reported in literature [15–17]. Laser beam properties, like polarization and coherence, as well as the angle of incidence to the target, affect the spatial periodic energy deposition that leads to the appearance of microstructures [16,18]. Generally speaking, the theory of the formation of microstructures is very complex [15,16]. Basically, fine microstructures are related to the Laser-Induced Periodic Surface Structure effect [16,18–20]. LIPSS is a phenomenon observed on semiconductors, metals and other materials which absorb laser radiation [16,18,20]. The LIPSS effects [16,18,19] are observed: (i) at low laser energy densities, as a consequence of spatially periodic melting induced by

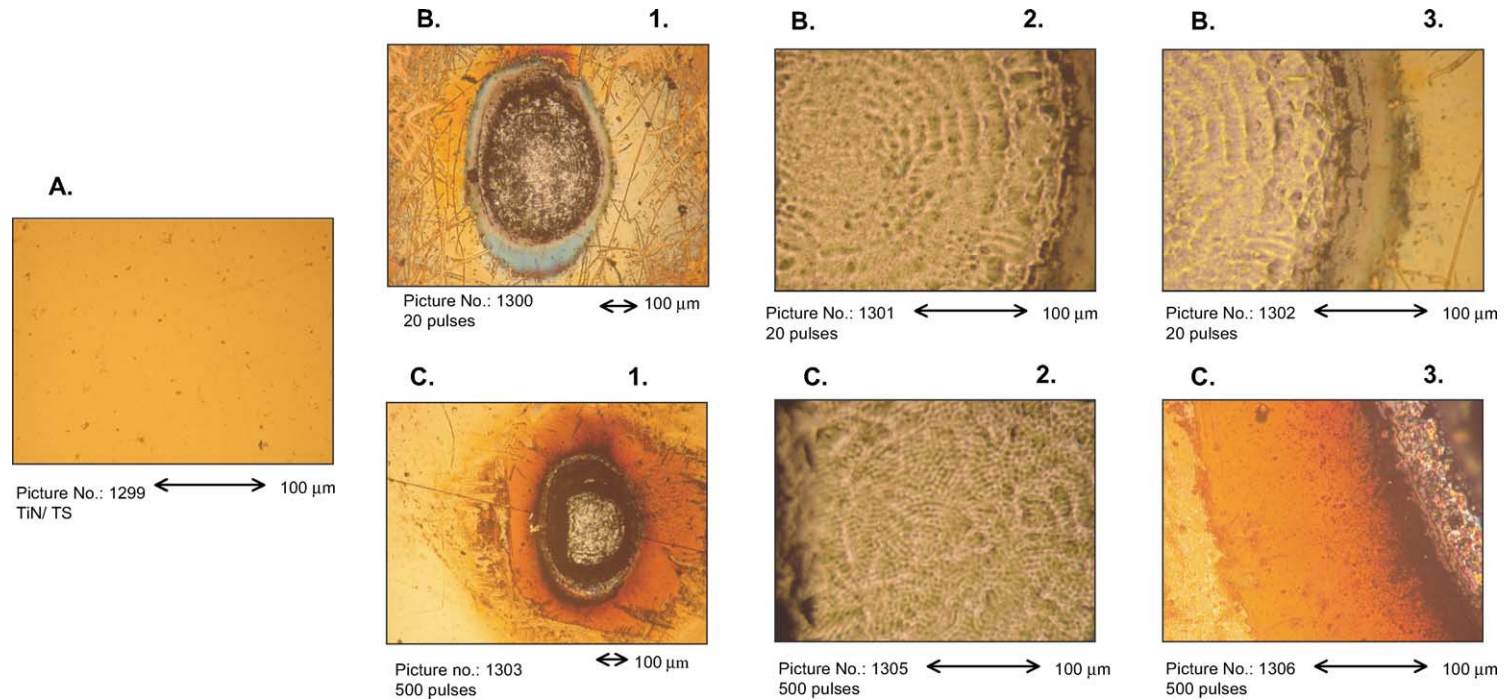


Fig. 5. KrCl laser-induced morphology changes of TiN coating (thickness, 1 μm)/Steel-AISI M2. Analysis was carried out by optical microscopy. Laser was operating in TEM_{00} mode; pulse width, 12 ns (FWHM)—Fig. 1B; energy density, 3.3 J/cm^2 . (A)—The view of TiN coating prior laser action; (B)—TiN coating after 20 laser pulse action ((B1–3)—entire spot, the center and periphery of the damage area, respectively); (C)—TiN coating after 500 laser pulses action ((C1–3)—entire spot, the center and periphery of the damage area, respectively).

inhomogeneous energy deposition into solid state targets (due to interference of incident and surface scattered waves), (ii) at medium laser energy densities, with induced capillary waves on the completely liquid surface, and (iii) at high energy densities, including formation of plasma plumes which screen target surfaces from incident light [16]. In the given regimes the cross-sectional contour of the ripples can vary significantly. The spatial period of the ripples, in some manner, is a function of the laser energy density used [16]. The spacing is defined by radiation residues produced at the solid/air interface or by the surface plasmon stimulated at the liquid/air interface [16]. Also, the role of intra- and inter-pulse feedback can be included in this consideration.

It should be emphasized that KrCl laser interaction with TiN coatings under the present exposure conditions causes the ignition of plasmas already during the first and all subsequent laser pulses.

Plasma formation, however, leads to distortion and dithering of the periodic structure of LIPSS [17]. In our case, the KrCl laser induced plasma jets on thin TiN films affect the development of periodic-ring structures on the target surface. In [26] we studied formation of regular structures on the surface of steel samples due to diffraction of UV-laser radiation (222 and 308 nm) introduced by optical elements (in particular, the aperture of a diaphragm). Correlations between the shape of the diaphragm and the LIPSS pattern were shown. Structures of mutually perpendicular bands were obtained with rectangularly shaped diaphragms, while circular diaphragm gave rise to concentric circles on the surface of steel samples. Moreover, the period of the structure was much longer than the laser wavelength and decreases with λ . In the present experiments with a circular diaphragm, we supposed that the ring-periodic structure. Fig. 5B2,3 can be explained by the formation of a diffraction pattern on the target. With the exception of a system of concentric circles in Fig. 5B2,3 and C2 only a thin disordered structure can be recognized. It can be concluded that in addition to LIPSS effects [18] diffraction effects of the laser radiation are also responsible for the formation of the observed complex surface structures, due to the finite aperture which contributes to the process.

Generally, TiN pulsed irradiation with the KrCl laser (3.3 J/cm^2) yields better coupling of the laser

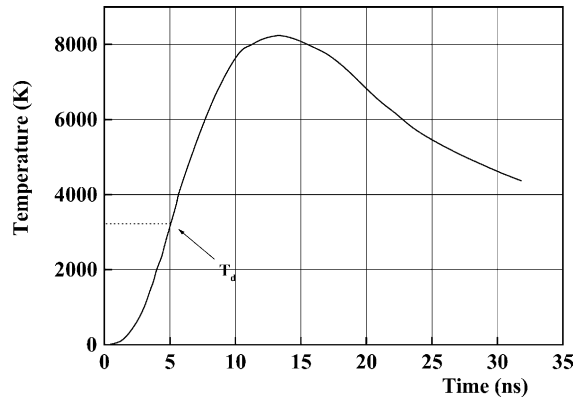


Fig. 6. Temperature surface variation of a sample during irradiation process with KrCl laser. (T_d denotes the decomposition temperature of the TiN coating).

energy with the target [21] than the TEA CO_2 laser (43.0 J/cm^2). This means also that a higher sample surface temperature is obtained. KrCl laser irradiation of TiN results in fast and intense target evaporation. It can also be assumed that the plasma induced above the target surface contains target atoms and ions. Processes like multiphoton ionization, photoionization from excited states, etc. are responsible for plasma ignition [22].

KrCl laser induced TiN surface temperatures versus time were also calculated using Eq. (1), as a function of the available energy density and pulse shape (Fig. 1B; $I_{\text{max}} = 280 \text{ MW/cm}^2$ and $A = 0.505$ [21]). The resulting plot of temperature versus time is represented in Fig. 6. A maximum of somewhat above 8000 K is achieved after about 12 ns (corresponding to about half of the pulse duration). The higher temperatures achieved with the KrCl laser than the TEA CO_2 laser are explained by the almost two-fold higher power density and considerably higher absorptivity in the UV spectral region.

The main error in these calculations is introduced by the uncertainty concerning absorptivities. For example, no data of A were found for TiN at $0.222 \mu\text{m}$ in the literature. It was therefore estimated using data from [21]. Calculated surface temperatures for bulk materials such as Ti, Si, Ge, Al, etc. [23–25], in contrast to this work, irradiated with lasers operating in the UV region can also be found in literature. The maximum calculated temperatures reported in these papers were in the range of 4500 K to about

6000 K, with laser intensities, however, typically lower than in our experiments.

4. Conclusion

A qualitative study of morphological changes on titanium nitride coatings deposited on high quality steels, induced either by a TEA CO₂ laser or by a KrCl laser is presented. It is shown that both lasers induce structural changes of the titanium nitride coating as well as of the steel-substrate. Laser energy densities of 43.0 J/cm² in the case of the TEA CO₂ laser and 3.3 J/cm² for the KrCl laser system were found to be sufficient for inducing surface modifications of the samples.

The energy absorbed from the CO₂ laser beam is mainly converted into thermal energy, causing melting, vaporization, and shock waves in the vapor and solid state material. Energy absorbed from the KrCl laser leads primarily to a fast and intense target evaporation. It can be assumed that the TEA CO₂ laser affects the target within a deeper zone than the KrCl laser due to the longer exposure time (pulse duration). In contrast, KrCl laser induced target effects are localized only near the target surface. The calculated temperatures of the target surfaces were 3940 K for the CO₂ laser and 8000 K for the KrCl laser. It should further be recognized that different mechanisms were responsible for plasma formation above the target. In the case of the TEA CO₂ laser, the plasma was ignited similarly as in the case of gas breakdown. In the case of the KrCl laser, it was initiated and developed in the form of evaporated metallic vapor consisting of target atoms and ions.

Qualitatively, the morphological modifications of the TiN target can be summarized as follows: (i) for both laser types, ablation of the TiN coating in the central zone of the irradiated area was recorded, (ii) appearance of a hydrodynamic feature, like resolidified droplets of the material, in the surrounding peripheral zone (cracking), in the case of TEA CO₂ laser was observed, and (iii) appearance of wave-like microstructures (periodic parallel fringes with a period of about 20 microns) in the case of KrCl laser. The formation of the wave-like microstructures is discussed in the context of laser-induced periodic surface structure effects and diffraction phenomena.

Color modifications upon laser irradiation of the target indicate possible chemical changes, like oxidation.

Acknowledgements

This research was financially supported by the Ministry of Science, Technologies and Development of the Republic of Serbia, Contracts no. 1995 and 2018 as well as by ISTC (Russia), Project no. 1206. The work is partially a result of cooperation in research in the field of Gas lasers and their applications between Vinča Institute of Nuclear Sciences, Belgrade, Serbia & Montenegro and the Institute of High Current Electronics (Siberian Branch, Russian Academy of Sciences), Tomsk, Russia (document no. 1629 from November 2001).

The authors have benefited considerably from discussions with professor Š.S. Miljanić, Faculty of Physical Chemistry, University of Belgrade.

We are also grateful to professor Dr. Peter Panjan from Jozef Stefan Institute, Ljubljana, Slovenia.

References

- [1] Goodfellow Catalogue, Goodfellow Cambridge Ltd., England, 2000.
- [2] M. Zlatanovic, B. Gakovic, A. Radivojevic, P. Drljaca, D. Dukic, S. Ristic, High-Power Laser Beam Interaction with the TiN Films Deposited onto HSS Substrates, 18th Summer School and International Symposium on the Physics of Ionized Gases (18th SPIG), Kotor, YU, Contributed Papers, 2–6 September 1996, pp. 229–232.
- [3] T.V. Kononenko, S.V. Garnov, S.M. Pimenov, V.I. Konov, V. Romano, B. Borsos, H.P. Weber, *Appl. Phys. A* 71 (2000) 627.
- [4] J. Bonse, H. Sturm, D. Schmidt, W. Kautek, *Appl. Phys. A* 71 (2000) 657.
- [5] V.F. Tarasenko, A.V. Fedenev, E.I. Lipatov, M.A. Shulepov, B.M. Gakovic, T.M. Nenadovic, Lj.T. Petkosvka, M.S. Trtica, Surface Modification of TiN Coating Induced by Pulsed TEA CO₂ and XeCl Laser, 21th Summer School and International Symposium on the Physics of Ionized Gases (21th SPIG), Sokobanja, YU, Contributed Papers, 26–30 August 2002, pp. 274–277.
- [6] M.S. Trtica, B.M. Gakovic, T.M. Nenadovic, *Proc. SPIE* 3885 (2000) 517.
- [7] B.M. Gakovic, M.S. Trtica, T.M. Nenadovic, B.J. Obradovic, *Thin Solid Films* 343–344 (1999) 269.
- [8] B.M. Gakovic, M. Trtica, T. Nenadovic, T. Gredic, *Appl. Surf. Sci.* 143 (1999) 78.

- [9] B.M. Gakovic, Z. Rakocevic, T.M. Nenadovic, D. Perusko, M.S. Trtica, S. Zec, *Solid State Phenom.* 61–62 (1998) 357.
- [10] M.S. Trtica, B.M. Gakovic, B.B. Radak, S.S. Miljanic, *Proc. SPIE* 4747 (2002) 44.
- [11] V.F. Tarasenko, E.H. Baksht, A.V. Fedenev, V.M. Orlovskii, A.N. Panchenko, V.S. Skakun, E.A. Sosin, *Proc. SPIE* 3343 (1998) 715.
- [12] M.S. Trtica, B.M. Gakovic, T.M. Nenadovic, M.M. Mitrovic, *Appl. Surf. Sci.* 177 (2001) 48.
- [13] Biljana M. Gakovic, *Modification of Low-Thickness Titanium Ceramics Induced by Pulsed Laser Radiation at 10.6 μm* , Ph.D. Thesis, University of Belgrade, Belgrade, 2001.
- [14] J. Hermann, C. Boulmer-Leborgne, I.N. Mihailescu, B. Dubreuil, *J. Appl. Phys.* 73 (1993) 1091.
- [15] A.J. Pedraza, J.D. Fowlkes, S. Jesse, C. Mao, D.H. Lowndes, *Appl. Surf. Sci.* 168 (2000) 251.
- [16] J.F. Young, J.E. Sipe, H.M. van Driel, *Phys. Rev. B* 30 (1984) 2001.
- [17] S. Clark, D.C. Emmony, *Phys. Rev. B* 40 (1989) 2031.
- [18] J.E. Sipe, J.F. Young, J.S. Preston, H.M. van Driel, *Phys. Rev. B* 27 (1983) 1141.
- [19] J.F. Young, J.S. Preston, H.M. van Driel, J.E. Sipe, *Phys. Rev. B* 27 (1983) 1155.
- [20] H.M. van Driel, J.E. Sipe, J.F. Young, *Phys. Rev. Lett.* 49 (1982) 1955.
- [21] J. Bonse, S. Baudach, J. Kruger, W. Kautek, *Proc. SPIE* 4065 (2000) 161.
- [22] J. Hermann, C. Viven, A.P. Carricato, C. Boulmer-Leborgne, *Appl. Surf. Sci.* 127–129 (1998) 645.
- [23] A.L. Thomann, C. Boulmer-Leborgne, C. Andreazza-Vignolle, P. Andreazza, J. Hermann, G. Blondiaux, *J. Appl. Phys.* 80 (1996) 4673.
- [24] V. Craciun, D. Craciun, *Appl. Surf. Sci.* 138–139 (1999) 218.
- [25] S. Amoroso, *Appl. Surf. Sci.* 138–139 (1999) 292.
- [26] V.F. Tarasenko, A.V. Fedenev, I.M. Goncharenko, N.N. Koval', E.I. Lipatov, V.M. Orlovskii, M.A. Shulepov, *Proc. SPIE* 4760 (2002) 93.